Short Communication

Effect of Chloride Diffusion on Corrosion Behavior of 304SS Steel in Simulated Concrete Solution under Carbonation Condition

Senlin Li[1], Weihang Miao[2], Ye Wu[1], Lupeng Liu[2], Zhiming Gao[2,]*

[1] Nanjing water conservancy research institute, Nanjing, Jiangsu 20029;
[2] Tianjin Key Laboratory of Composite & Functional Materials, School of Materials Science and Engineering, Tianjin University, Tianjin, 300350, China
[*]E-mail: gaozhiming@tju.edu.cn

The corrosion behavior of 304 stainless steel reinforced concrete in the simulated seawater environment is studied using the ion diffusion method to accelerate the carbonation process of the simulated concrete stainless steel system. The results show that the concrete has a strong ability to protect the internal stainless steel, and the stainless steel is not susceptible to local corrosion before the carbonation process of concrete is completed. In the early stage of the severe carbonation test, with the increase in immersion time, the capacitive semicircle diameter of the EIS plot is changed slightly. At the later stage of the severe carbonation test, the capacitive semicircle diameter decreases significantly, which indicates the damage and corrosion of passive film on the stainless steel surface. When the stainless steel remains passive, its corrosion potential is positive. However, the corrosion potential of stainless steel decreases rapidly when the corrosion process is being occurred. The morphology of the surface of specimens after the severe carbonation test shows that almost all metal surfaces of stainless steel in concrete are corroded after complete carbonation.

1. INTRODUCTION

The main factors affecting the durability of concrete system are physical and chemical corrosion. The corrosion of reinforcement in concrete is a form of chemical reaction, which is usually considered as one of the important reasons leading to the failure of reinforced concrete structure. The corrosion of steel is mainly caused by CO_2 and chloride [1]. Under normal conditions, the surface of ordinary steel bar is in a passive state, and there is a thin iron oxide film on the surface. When chloride ion reaches a

certain concentration, the passive state of steel bar will be damaged. The carbonation of concrete is mainly caused by the action of CO_2 in the atmosphere. The pH of concrete decreases from 13 to 9. If all calcium hydroxide in concrete is carbonated, the pH can be reduced to 8.3.

In harsh environment, the use of stainless steel reinforcement is an economic and reliable scheme, which can ensure the durability of concrete structure under certain conditions[2]. The research shows that the corrosion resistance of 304SS passive film decreases with the decrease of pH value and the increase of Cl^- concentration in simulated environment with different pH value and Cl^- concentration. The corrosion environment changes caused by concrete carbonization process and Cl^- enrichment will have an important impact on 304SS. The stability of 304SS passive film decreases and the tendency of corrosion increases [3].

The effect of Cl^- on the corrosion behavior of metals has long been concerned by corrosion scientist [4-7]. Corrosive Cl^- can affect the pitting corrosion behavior of stainless steel and lead to the failure of stainless steel reinforcement. As we all know, pitting is characterized by two successive stages: the initiation of pitting and the stable development of pitting[6].

For stainless steel[8] concrete, the effect of carbonization process on its corrosion resistance needs to be explored. In this paper, the corrosion behavior of 304SS stainless steel in simulated carbonation process with reduced pH was studied by using concrete system.

2. EXPERIMENTAL METHODS

The chemical composition of 304SS stainless steel used for conducting experiments is shown in the Table 1.

Table 1. Main chemical composition of 304 stainless steel (mass fraction)

Steel	Cr	Ni	Mo	N	Mn	Fe	PREN
304SS	18	8	0.05	0.1	<2	balance	19

304SS is cut into standard sample dimension of 10 mm × 10 mm × 1 mm. After rust removal, the back of the sample is welded with copper wire and sealed with PVC pipe and epoxy resin. The sample is reserved until the epoxy resin is completely cured and is used for corrosion potential and electrochemical impedance spectroscopic studies. Another 4 cm × 30 cm 304SS stainless steel sheet is processed for surface potential scanning after severe carbonization experiment.

Use 150, 400, 800, 1500, and 2000 mesh water sandpaper to grind the sealed sample 10 mm × 10 mm × 1 mm step by step with the use of a 0.5 micron diamond polishing agent to polish. Then clean the surface of the sample with distilled water and absolute alcohol, dry it with a blower, and put it into a drying dish for later use.

The 4 cm × 30 cm 304SS stainless steel sheet is packaged with concrete, and the concrete thickness is controlled at about 2 mm to obtain samples and test blocks.

To understand the electrochemical information with regards to changes in the surface morphology of stainless steel after corrosion of stainless steel concrete structure, carbonation is simulated using an acid solution in the diffusion accelerated corrosion process where the samples are immersed in saturated sodium chloride solution. To accelerate the carbonation process of concrete, dilute hydrochloric acid is added every 24 h to make sure the external solution maintains a pH of 5.

Electrochemical impedance spectroscopy (EIS) and open circuit potential (OCP) are tested once each day. The three-electrode system is used while performing the test. The saturated calomel electrode is used as the reference electrode, the platinum electrode is used as the counter electrode, and the lead-out wire from the test sample is used as the working electrode. To minimize the solution resistance and ensure the accuracy of the test, both the reference electrode with salt bridge and the platinum electrode are placed in the saturated sodium chloride environment. An electrochemical workstation (PARSTAT 2273) is used to record EIS and OCP where OCP is measured using the amplitude of the AC sine wave signal of 10 mV in the scanning frequency range of 100 kHz to 10 mHz. The test data are fitted with zsimpwin and plotted with origin.

3. RESULT AND DISCUSSION

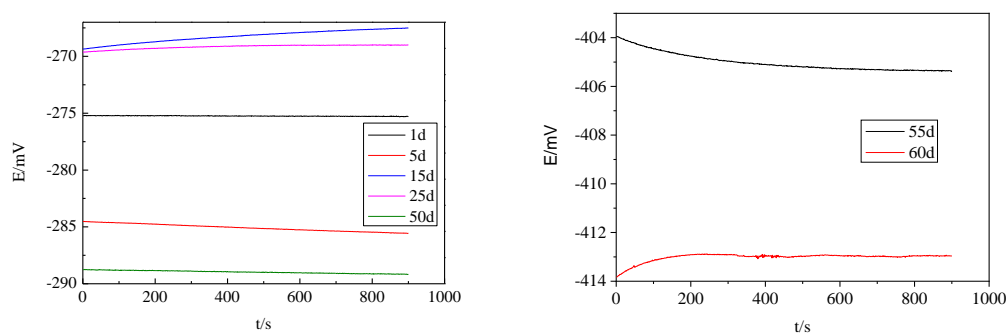*3.1 Open circuit potential of simulated concrete solution test at different time*

Figure 1. Open circuit potential of 304 stainless steel in simulated concrete pore solution after different immersion time
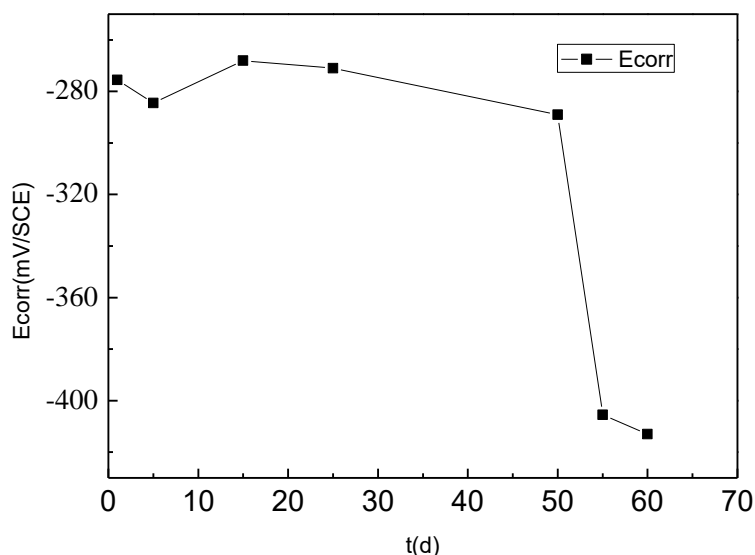
Figure 2. Stable corrosion potential of 304 stainless steel in simulated concrete pore solution with time

From the open circuit potential, it can be seen that till the 50th day the open circuit potential is always found close to -280 mV[9]. However, on the 55th day and 60th day of testing, the open circuit potential shows a huge change reducing it below -400 mV. Therefore, it is corroborated that between the 50th day and 55th day, the passive film of the sample is damaged and the corrosion is intensified. On the 60th day, the corrosion is further aggravated.

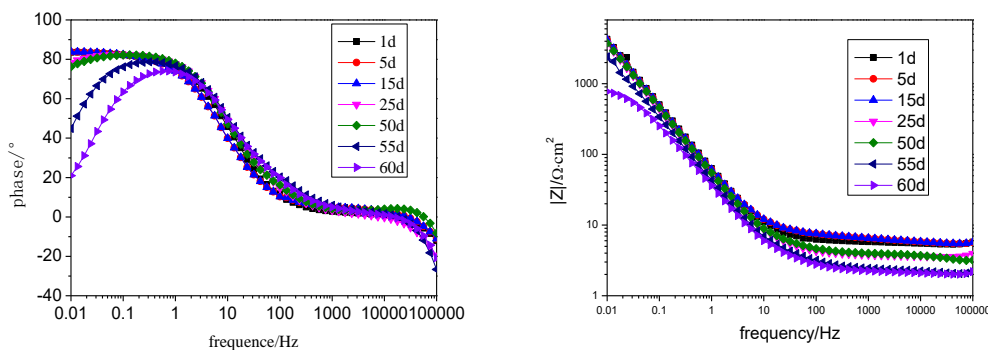*3.2 Impedance spectrum characteristics of severe carbonation*
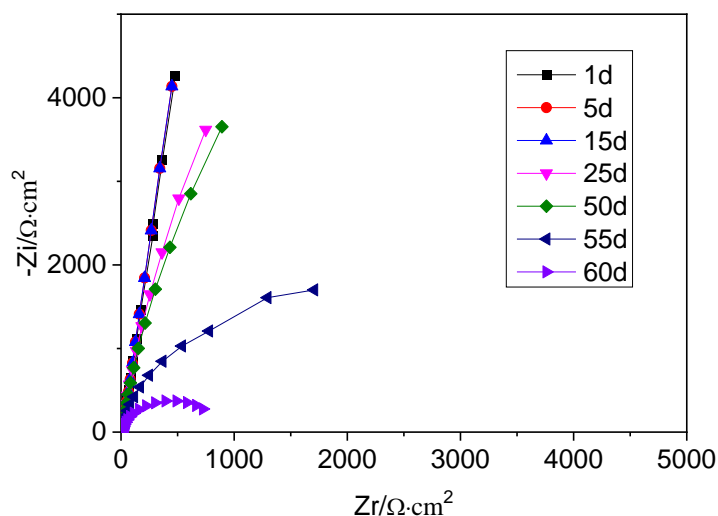
Figure 3. The EIS of 304 stainless steel in simulated concrete pore solution after different immersion time
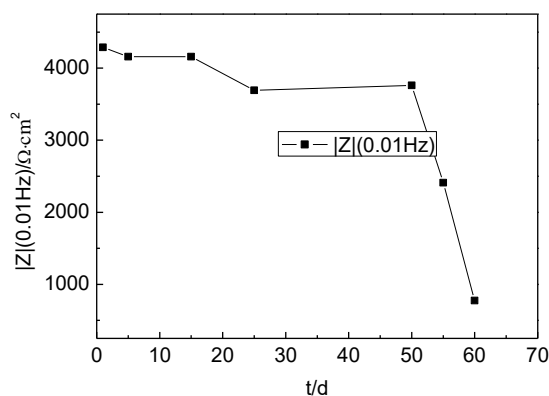

Figure 4. $|Z_{0.01Hz}|$ of 304 stainless steel in simulated concrete pore solution with time

It can be seen from the impedance spectra shown in Fig. 3 that with the increase in immersion time, the diameter of the impedance semicircle gradually decreases [10,11]. It is speculated that the decrease in concrete protective resistance is caused by the concrete carbonation and the accelerated dissolution of the passive film by chloride ions.[12] However, the impedance at 55th day and 60th day is much less compared to other treatment times, which validates that the damage and corrosion of passive film on stainless steel surface occur during this period[13]. These results are found consistent with the change in open circuit potential. Therefore, the damage and corrosion of passive film on stainless steel surfaces can be detected by the change in open circuit potential[14].

Therefore, through electrochemical impedance spectroscopy (EIS) and Open circuit potential (OCP) of 304 stainless steel and the accelerated corrosion experiments of real stainless steel concrete, the potential change of stainless steel [15] is estimated. Initially, the 304 stainless steel concrete is found to be stable having corrosion potential in the range of -200 mV. Since the penetration rate of chloride ions is much faster than the carbonation rate of concrete owing to the joint action of tide and transpiration, the chloride ion concentration rises rapidly which results in a drop in the open circuit potential to about -300 mV. When the carbonation process occurs for a longer period till it reaches the interface between stainless steel and concrete, the pH value of concrete pore liquid decreases rapidly and subsequently, the potential of stainless steel also decreases. When carbonization occurs at the interface between steel and concrete, the passive film over stainless steel is destroyed and corroded in a short time

leading to a potential drop to -400 mV. Therefore, detecting the open circuit potential of stainless steel is one of the scientific methods to judge whether the reinforcement is being corroded or not.

3.3 Surface potential scanning of severe carbonation experiment

The surface potential of the stainless steel concrete sample is scanned after 60 days of immersion. The reference electrode is the saturated calomel electrode. Here, the reference electrode is used to measure the potential every 1 cm on the sample surface. The reference electrode is closely attached to the surface of the measured click area to reduce the potential influence of other areas. According to the size of the stainless steel sheet, the scanning quantity is 4×30. The potential distribution is shown in Fig. 5.

The upper part of Fig. 5 is far away from the wire welding part and is also the lower end of the glass tube container. The lower part is the wire welding part, which is placed at the upper end in a glass tube container. The degree of corrosion degree is higher for the part with low potential and lower for the area with higher potential. The reason for the uneven occurrence of corrosion validated from this figure is due to the distribution of oxygen. As mentioned above, the consumption of oxygen in the diffusion process of chloride ions results in the solution of passive film, so it is difficult for oxygen to diffuse to the bottom of the glass tube. Therefore, the dissolution rate of the passive film is fast leading to the poor corrosion resistance of the passive film. On the top of the glass tube, as the oxygen in the air is can easily diffuse, the corrosion resistance of the passive film is good. When the corrosion process of the stainless steel begins, this area acts as the cathode area and so, almost no corrosion occurs [16]. Therefore, the upper potential of the sample is higher. That is why the lower end of the figure shows a higher potential and the upper end shows a lower potential.
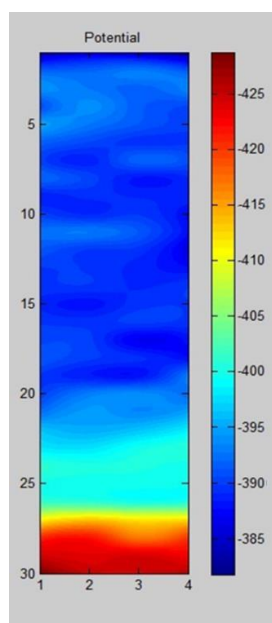

Figure 5. The surface potential scan image of 304SS concrete specimen after 60 days of immersion

Similarly, this method can be used to evaluate whether the stainless steel is corroded on site. Combined with the above potential changes, if there is a local low potential and peripheral high potential, the local corrosion of stainless steel at the low potential can be considered.

The stainless steel which is reinforced inside the concrete is observed by breaking the external concrete. The corrosion of stainless steel is not serious at this time and obviously, the corrosion occurs only to the lower end of the immersion. There is an apparent accumulation of white corrosion products is seen, which are oxides of nickel. Combined with the scanning of surface potential, it can be seen that the upper end of immersion have higher potential where the stainless steel surface is whiter and smoother than other surfaces, and the other parts having lower potential are found black in color[17]. The micrograph of the blackened part observed at 200× magnification is shown in Fig. 6.

Figure 6. The surface morphology of 304SS after accelerated corrosion of stainless steel concrete after 60 days of immersion

From Fig. 6, it is clear that all surfaces covered by concrete have been corroded. The darker part of the stainless steel has obvious pitting, and there are many pits that have the shape of shallow pits [18]. Therefore, surface potential scanning is one of the feasible methods to evaluate whether there is corrosion in someplace. The early corrosion of stainless steel can be found by observing the low potential value.

4. CONCLUSION

1. The concrete has a strong ability to protect the internal stainless steel, and the stainless steel will not undergo local corrosion before the concrete carbonization process is completed.

2. In the early stage of the severe carbonation test, with the increase in immersion time, the capacitive semicircle diameter of EIS changed slightly. However, at the later stage of the severe carbonation test, the capacitive semicircle diameter decreases rapidly, validating the passive film on the stainless steel surface is destroyed and is being corroded.

3. Based on the experiment results, the relationship between electrode potential and corrosion behavior of stainless steel is established. When the stainless steel remains passivated, its electrode potential is higher. However, the electrode potential of stainless steel decreases rapidly when corrosion occurs.

Int. J. Electrochem. Sci., 16 **(2021)** Article ID: 21095

8

References

1. V. T. Ngala, C. L. Page and M. M. Page, *Corros. Sci.*, 45(2003)1523.
2. X. G. Feng, X. Y. Lu, Y. Zuo, N. Zhuang and D. Chen, *Corros. Sci.*, 103(2016)223.
3. W. H. Miao, W. B. Hu, Z. M. Gao, X. G. Kong, R. Zhao and J. W. Tang, *Journal of Chinese Society of Corrosion and Protection*, 36(2016)543.
4. D. H. Xia, R. K. Zhu, B. Yashar, J. L. Luo and C. J. Lin, *J. Electroanal. Chem.*, 744(2015)77.
5. A. Pardo, E. Otero, M. C. Merino, M. D. López, M. V. Utrilla and F. Moreno, *Corrosion*, 56(2000)411.
6. S. Fajardo, D. M. Bastidas, M. Criado and J. M. Bastidas, *Electrochim.Acta*, 129(2014)160.
7. P. C. Pistorius and G. T. Burstein, *Corros. Sci.*, 36(1994)525.
8. P. C. Pistorius and G. T. Burstein, *Philos. Trans. Roy. Soc.*, 341(1992)531.
9. G. Ruhi, O. Modi and I. Singh, *Corros. Sci.*, 51 (2009) 3057.
10. Z. Wu, J. G. Zhao , S. J. Zhang and J. B. Yang, *Int. J. Electrochem. Sci.*, 14(2019)8039.
11. H. Luo, H. Su, C. Dong and X. Li, *Applied Surface Science*, 400(2017)38.
12. C. Liu, Q. Bia, A. Leyland and A. Matthews, *Corros. Sci.*, 45 (2003) 1257.
13. E.C. Souzaa, S.M. Rossittib and J.M.D.A. Rolloa, *Mater, Charact.*, 61 (2010) 240.
14. A. Bautista, G. Blanco, F. Velasco, A. Gutiérrez, L. Soriano, F.J. Palomares and H.
15. Takenouti, *Corros. Sci.*, 51 (2009) 785.
16. C. Chen, J. W. Zuo and Y. J. Wang, *Int. J. Electrochem. Sci.*, 15(2020)4049.
17. J. Ozbolt, E. Sola and G. Balabanic, *Materials and Corrosion*, 68(2017)622.
18. H. E. Jamil, M. Montemor, R. Boulif, A. Shriri and M. Ferreira, *Electrochim.Acta*, 48 (2003)
19. 3509.
20. L. Freire, M. J. Carmezim, M. G. S. Ferreira and M. F. Montemor, *Electrochim. Acta*, 56(2011)5280.